Brain Image Registration using Cortically Constrained Harmonic Mappings

Anand Joshi[1], **David Shattuck**[2], **Paul Thompson**[2], and **Richard Leahy**[1]

Anand Joshi: ajoshi@sipi.usc.edu; David Shattuck: shattuck@loni.ucla.edu; Paul Thompson: thompson@loni.ucla.edu; Richard Leahy: leahy@sipi.usc.edu

[1]Signal and Image Processing Institute, University of Southern California, Los Angeles 90089, USA

[2]Laboratory of Neuro Imaging, UCLA school of Medicine, Los Angeles, CA 90095, USA

Abstract

Volumetric registration of brains is required for inter-subject studies of functional and anatomical data. Intensity-driven registration typically results in some degree of misalignment of cortical and gyral folds. Increased statistical power in group studies may be achieved through improved alignment of cortical areas by using sulcal landmarks. In this paper we describe a new volumetric registration method in which cortical surfaces and sulcal landmarks are accurately aligned. We first compute a one-to-one map between the two cortical surfaces constrained by a set of user identified sulcal curves. We then extrapolate this mapping from the cortical surface to the entire brain volume using a harmonic mapping procedure. Finally, this volumetric mapping is refined using an intensity driven linear elastic registration. The resulting maps retain the one-to-one correspondence between cortical surfaces while also aligning volumetric features via the intensity-driven registration. We evaluate performance of this method in comparison to other volumetric registration methods.

1 Introduction

Morphometric and functional studies of human brain require that neuro-anatomical data from a population be normalized to a common template. The goal of registration methods is to find a map that assigns a correspondence from every point in a subject brain to a corresponding point in the template brain. Since cytoarchitectural and functional parcellation of the cortex is intimately related to the folding of the cortex, it is important when comparing cortical anatomy and function in two or more subjects that the cortical surfaces are accurately aligned. However, it is a non-trivial problem to find a map from a subject brain to a template brain which maps grey matter, cortical surface and white matter to the corresponding regions in the template brain.

Volumetric brain image registration methods [1–8] find a deformation field that aligns one volume to another using intensity values, ideally to establish a diffeomorphism between the two brain image volumes. Using intensity only typically results in accurate registration of subcortical structures, but poorer alignment of cortical features. Information such as landmark points, curves and surfaces can be incorporated as additional constraints in an intensity-based warping method to improve alignment of the cortical surface [9–15]. For

example, landmarks, curves [13] and image matching [12] can be applied in a hierarchical manner in a large deformation framework to ensure generation of diffeomorphisms [16, 17]. Hybrid methods such as HAMMER [18] implicitly incorporate surface as well as volume information in the alignment.

An alternative approach for studying the cortex is to use a surface based analysis. A number of surface-based techniques have been developed for inter-subject registration of cortices. These techniques involve flattening the two cortical surfaces to a plane [19, 20] or to a sphere [21, 22] and then registering the two surfaces in the intermediate flat space [23, 21] or in the intrinsic surface geometry via covariant derivatives [24, 25]. These approaches can be automatic [26, 23], or semi-automatic using sulcal landmarks [24, 25]. Although progress has been made towards automatic surface registration [26, 23], accurate fully automatic registration remains a challenge.

The main advantage of a purely surface based method is that the cortical surface can be modeled at high resolution, producing a precise point correspondence between cortical surfaces such that sulcal landmarks are aligned. However, these methods do not define a volumetric correspondence, so one is restricted to analyzing only cortical effects. The goal of this paper is to develop a registration method in which we retain the advantage of accurate cortical and sulcal alignment within a fully 3D volumetric registration. This approach takes advantage of strengths of both types of methods: the ability of surface based methods to accurately align complicated folding patterns and the ability of volumetric intensity based methods to align internal subcortical structures.

The algorithm we develop consists of three steps: (i) extraction, labelling and alignment of the cortical surfaces, (ii) extrapolation of the surface mapping to the volume using harmonic maps, and (iii) refinement of the volumetric map using an intensity driven linear elastic warp. We describe the cortical surface extraction and alignment procedure in Section 3. The result of this alignment is a 2D parameterization of the two cortical surfaces in which sulcal landmarks are aligned. The extrapolation of these parameterizations to three dimensions is then computed using harmonic mapping, an approach which we review below. Finally, we use an intensity-driven linear elastic warp as described in Section 5.

A number of existence, uniqueness, and regularity results have been proven for harmonic maps [27–29]. Harmonic maps and their generalized counterparts, p-harmonic maps [30], have been used for various applications such as surface parameterization and registration [31, 32], [20] and image smoothing [33]. Wang, et al. [34] describe a method for volumetric mapping of the brain to the unit ball $B(0, 1)$. In recent papers, Joshi, et al. [35][36] described a method for combined surface and volume registration that used a similar three step procedure. In that case, the harmonic mapping used an intermediate unit ball representation which has the advantage of allowing the cortical surfaces to flow within each other. The distortion introduced in the intermediate space was corrected by associating a Riemannian metric with that representation. The limitation of this approach is that by using the map to the unit ball, the method is restricted to mapping only the cerebral volume contained within the cortical surface. Here we avoid this restriction by computing the harmonic map directly in Euclidean space so that the entire brain volume can be registered. We do this by fixing the

correspondence between all points on the cortical surface rather than just the sulcal curves as in [35][36]. Since the map between the cortical surfaces is fixed, there is no longer a need for the intermediate spherical representation. While this approach places a more restrictive constraint on the mapping of the surface, in practice we see little difference between the two methods in the mapping of the interior of the cerebrum.

2 Problem Statement and Formulation

The registration problem is formulated in the following manner. We start by aligning the cortical surfaces, semi-automatically, using sulcal landmarks. We then use harmonic maps to extrapolate this surface mapping to the entire cortex. It is nontrivial to extend the surface map to the full 3D volumetric map due to large inter-subject variability in sulcal structures and the complicated folding pattern of the sulci. For example, the widely used linear elastic or thin-plate spline registration methods based on landmarks are not useful for this extrapolation due to their tendency to generate folds [37]. Harmonic maps, on the other hand, are particularly suitable for this task since they tend to be bijective provided that the boundary (the cortical surface in this case) is mapped bijectively [38, 34]. The volumetric point correspondence obtained from these harmonic maps is then refined further using volumetric registration based on image intensity.

Given two 3D manifolds M and N representing brain volumes, with M_1, M_2 and N_1, N_2 representing surfaces corresponding to cortical grey/white matter and grey/CSF boundaries, we want to find a map from M to N such that (i) M_1, the grey/white matter surface of M, maps to N_1, the grey/white matter surface of N; (ii) M_2, the grey/CSF surface of M, maps to N_2, the grey matter/CSF surface of N; and (iii) the intensities of the images in the interior of M and N are matched. The surfaces, M_1, M_2 and N_1, N_2, are assumed to have a spherical topology. We solve the mapping problem in three steps:

1. Surface matching which computes maps between surface pairs - the cortical surfaces and the grey matter/csf surfaces of the two brains, with sulcal alignment constraints (Section 3);

2. extrapolation of the surface map to the entire cortical volume. This is done by computing a harmonic map between M and N subject to a surface matching constraint (Section 4), and

3. Refinement of the harmonic map on the interiors of M and N to improve intensity alignment of subcortical structures (Section 5).

3 Surface Registration

Assuming as input two T1-weighted MRI volumes corresponding to the subject and the template, cortical surfaces are extracted using the BrainSuite software [39]. BrainSuite includes a six stage cortical modeling sequence. First the brain is extracted from the surrounding skull and scalp tissues using a combination of edge detection and mathematical morphology. Next the intensities of the MRI are corrected for shading artifacts. Each voxel in the corrected image is labeled according to tissue type using a statistical classifier. Co-registration to a standard atlas is then used to automatically identify the white matter

volume, fill ventricular spaces and remove the brain stem and cerebellum, leaving a volume whose surface represents the outer white-matter surface of the cerebral cortex. It is likely that the tessellation of this volume will produce surfaces with topological handles. Prior to tessellation, these handles are identified and removed automatically using a graph based approach. A tessellated isosurface of the resulting mask is then extracted to produce a genus zero surface which is subsequently split into two cortical hemispheres. These extracted surfaces are hand labeled with 23 major sulci on each cortical hemisphere according to a sulcal labeling protocol with established intra- and inter-rater reliability [39]. Grey matter/CSF surfaces are extracted similarly except that topology correction was done manually by morphological operation tools in BrainSuite.

One method for alignment of surfaces with sulcal constraints is based on intrinsic thin-plate spline registration [25]. In that method, a deformation field is found in the intrinsic geometry of the cortical surface, which results in the required sulcal alignment. Covariant derivatives with the metric for the flat coordinates are used in order to make the deformation independent of the flat representation. The method requires the surfaces to be re-sampled on a regular or semi-regular grid in the flat space for discretization of the covariant derivatives. In addition to the loss of resolution, this leads to an added computational cost of interpolations for the re-sampling brain surface in the flat space. To overcome this problem, we follow a registration method described in [40] which registers surfaces by simultaneously parameterizing and aligning homologous sulcal landmarks. In order to generate such a parameterization with prealigned landmarks, we model the cortical surface as an elastic sheet by solving the linear elastic equilibrium equation in the geometry of the cortical surface using the form:

$$\mu \Delta \phi + (\mu + \lambda) \nabla (\nabla \cdot \phi) = 0, \quad (1)$$

where μ and λ are Lamé's coefficients and φ denotes 2D coordinates assigned to each point on the surface. The operators   and ∇ represent the Laplace-Beltrami and covariant gradient operators, respectively, with respect to the surface geometry. The solution of this equation can be obtained variationally by minimizing the integral on the cortical surface [41]:

$$E(\phi) = \int_S \frac{\lambda}{4} (\mathrm{Tr}((D\phi)^T + D\phi))^2 + \frac{\mu}{2} \mathrm{Tr}(((D\phi)^T + D\phi)^2) dS, \quad (2)$$

where $D\phi$ is the covariant derivative of the coordinate vector field φ. The integral $E(\phi)$ is the total *strain energy*. Though the elastic equilibrium equation models only small deformations, in practice we have found that it is always possible to get a flat map of the cortex by setting the parameters μ = 10 and λ = 1.

Let ϕ_M and ϕ_N denote the 2D coordinates to be assigned to corresponding hemispheres of *M* and *N* brains respectively. We then define the Lagrangian cost function $C(\phi_M, \phi_N)$ as

$$C(\phi_M, \phi_N) = E(\phi_M) + E(\phi_N) + \sigma^2 \sum_{k=1}^{K} (\phi_M(x_k) - \phi_N(y_k))^2, \quad (3)$$

where $\varphi_M(x_k)$ and $\varphi_N(y_k)$ denote the coordinates assigned to the set of K sulcal landmarks $x_k \in M$, $y_k \in N$ and σ^2 is a Lagrange multiplier. The cost function is then discretized in the intrinsic surface geometry by finite elements as described in [40] and minimized by conjugate gradients. This procedure is applied to both the inner and outer pairs of cortical surfaces M_1, N_1 and M_2, N_2 to achieve a bijective point correspondence between each pair. This surface alignment and parameterization procedure is illustrated for the inner grey/white cortical boundary in Fig. 1.

4 Harmonic Mapping

The surface registration procedure described in Section 3 sets up a point to point correspondence between the pairs of surfaces M_1, M_2 and N_1, N_2. As noted earlier, treating these surfaces as landmarks is not helpful since they are highly convoluted and finding a volumetric diffeomorphism consistent with the surface map is non-trivial. One approach that can achieve such a diffeomorphism is to compute a harmonic map. A harmonic map $u = (u^1, u^2, u^3)$ from 3D manifold M to 3D manifold N is defined as the minimizer of the harmonic energy [29],

$$E_h(u) = \frac{1}{2} \int_M \sum_{i=1}^{3} \sum_{\alpha=1}^{3} \left(\frac{\partial u^\alpha(x)}{\partial x^i} \right)^2 dV. \quad (4)$$

Note that (4) is quadratic in u^α and that the summands are decoupled with respect to α. Consequently the harmonic energy $E_h(u)$ can be separately minimized with respect to each component u^α, $\alpha \in \{1, 2, 3\}$.

We compute the minimizer of $E_h(u)$ using a conjugate gradient method with Jacobi preconditioner. The mapping of the two surfaces computed in the previous sections act as constraints such that M_1 maps to N_1 and M_2 maps to N_2. This harmonic mapping extrapolates the surface mappings to the entire volume such that the surface alignments are retained.

5 Volumetric Intensity Registration

The previous harmonic mapping step matches inner and outer cortical boundaries by computing a large deformation of the template brain to obtain a constrained bijective mapping between the two brain volumes. However, this map uses only the shape and not the MRI intensity values. Consequently we need a final small scale deformation to refine the mappings so that subcortical and extra-cerebral structures are also aligned. To compute this refinement we use a linear elastic registration method [6] as described below. We impose the constraint that cortical boundaries remain stationary during this refinement so that the cortical correspondence is retained.

Let $f_M(x)$ denote the MRI intensity value at location $x = (x_1, x_2, x_3)^t$ for the brain M and let $f_N(x)$ denote the MRI intensity value at location $x = (x_1, x_2, x_3)^t$ for the brain N. In order to find a smooth deformation field $d = (d_1, d_2, d_3)^t$ such that the mean squared error between MRI intensity values of the two brains $f_M(x + d)$ and $f_N(x)$ is minimized, we minimize the cost function

$$C(d) = \|Ld\|^2 + \alpha \|f_M(x+d) - f_N(x)\|^2 \quad (5)$$

$$\text{subject to } d(s) = 0 \text{ for } s \in \partial M_1, \partial M_2$$

where $L = \nabla_2 + \mu\nabla(\nabla\cdot)$ denotes the Cauchy-Navier elasticity operator in M. By imposing the constraint (6) on the deformation field, we ensure that the surface alignment is not affected. Assuming that the deformation d is small compared to the rate of change of f_M, then using a Taylor series approximation, we have $f_M(x + d) \approx f_M(x) + \nabla f_M(x) \cdot d$. Substituting this approximation in (5) and (6), we get

$$C(d) \approx \|Ld\|^2 + \alpha\|\nabla f_M(x) \cdot d(x) + f_M(x) - f_N(x)\|^2 \quad (6)$$

$$\text{subject to } d(s) = 0 \text{ for } s \in \partial M_1, \partial M_2$$

Note that this is a quadratic cost function and can again be minimized by the conjugate gradient method. We use a preconditioned conjugate gradient method with Jacobi preconditioner.

This final refinement completes the surface-constrained registration procedure. While there are several steps required to complete the registration, each step can be reduced to either a surface or a volume mapping cast as an energy minimization problem with constraints, and can be effectively computed using a preconditioned conjugate gradient method. Thus, the entire procedure can be completed efficiently.

6 Results

In this section we demonstrate the application of the surface constrained registration procedure to T1-weighted MR brain images. We took the genus zero cortical mask, the tessellated cortical surface, the sulcal labels, and the original image intensities for two brains and applied our alignment procedure as described above. Shown in Fig. 3 are three orthogonal views of a subject before and after alignment to the template image. Note that before alignment the surfaces of the subject and template are clearly different, while after matching the subject surface almost exactly matches the morphology of that of the template. However, since at this point we do not take the image intensities into account, the interior structures are somewhat different. Following the final intensity-based alignment procedure the interior structures, such as the subject ventricles, are better matched to those of the template. There is no gold standard for evaluating the performance of registration algorithms such as the one presented here. However, there are several properties that are desirable for any such surface and volume registration algorithm. Our method for evaluating the quality of our registration results is based on the following two desirable properties:

1. Alignment of the cortical surface and sulcal landmarks. We expect the sulcal landmarks to be accurately aligned after registration and for the two surfaces to coincide.

2. Alignment of subcortical structures. We also expect the boundary of subcortical structures (thalamus, lateral ventricles, corpus callosum) to be better aligned after coregistration than before.

For evaluating performance with respect to the first property, we compared the RMS error in sulcal landmark registration for pair-wise registration of a total of five brain volumes. We performed a leave-one-out validation in which we removed one sulcus from the set of curves to be aligned and then computed the RMS error in alignment for that sulcus; the procedure was repeated for each sulcus in turn. The mean squared distance (misalignment) between the respective sulcal landmarks was 11*mm* using a 5th order intensity-only registration with AIR [3] and 11.5*mm* for the HAMMER algorithm [18, 42], which uses a feature vector based on a set of geometric invariants. The RMS error for our approach was 2.4*mm*. The difference reflects the fact that our approach explicitly constrains these sulcal features to match, which AIR and HAMMER do not.

For the second property, we used manually labeled brain data from the IBSR database at the Center for Morphometric Analysis at Massachusetts General Hospital. These data include volumetric MRI data and hand segmented and labeled structures. We first traced the 23 sulci for each brain. We then applied the HAMMER software and our method using the sulcal landmarks as additional constraints. To evaluate accuracy, we computed the Dice coefficients for each structure, where the structure names and boundaries were taken from the IBSR database. The Dice coefficient measures overlap between any two sets representing regions S_1 and S_2, and is defined as $\dfrac{2|S_1 \cap S_2|}{|S_1|+|S_2|}$ where $|\cdot|$ denotes size of the region [43]. A comparison of the Dice coefficients is shown in Table 6, where we show Dice coefficients for our method before and after application of the final intensity-based alignment step.

These results show superior alignment of cortical grey matter while HAMMER achieves superior alignment of subcortical structures. These results appear reasonable since HAMMER uses boundary information throughout the volume as part of the feature vector and thus can produce superior alignment of subcortical boundaries than our method which is based solely on image intensity. Conversely, the more specific cortical information in our approach leads to superior results in the cortical grey matter. Based on these preliminary observations, we believe that the approach described here could be appropriate for use in applications where cortical alignment may be of particular importance such as morphometric studies of cortical thinning, fMRI studies and analysis of DTI fiber tract data.

Acknowledgment

References

1. Talairach, J.; Tournoux, P. Co-planar Stereotaxic Atlas of the Human Brain: 3-Dimensional Proportional System - an Approach to Cerebral Imaging. Thieme Medical Publishers; New York, NY: 1988.

2. Ashburner, J.; Friston, K. Spatial normalization. In: Toga, A., editor. Brain Warping. Academic Press; 1999. p. 27-44.

3. Woods RP, Grafton ST, Holmes CJ, Cherry SR, Mazziotta JC. Automated image registration: I. General methods and intrasubject, intramodality validation. Journal of Computer Assisted Tomography. 1998; 22:139–152. [PubMed: 9448779]

4. Hill DLG, Batchelor PG, Holden M, Hawkes DJ. Medical image registration. Phys. Med. Biol. 2001 Mar; 46(4):R1–R45. [PubMed: 11277237]

5. Christensen GE, Rabbitt RD, Miller MI, Joshi SC, Grenander U, Coogan TA, Essen DCV. Topological properties of smooth anatomic maps. IPMI. 1995:101–112.

6. Christensen GE, Rabbit RD, Miller MI. Deformable templates using large deformation kinematics. IEEE Transactions on Image Processing. 1996; 5(10):1435–1447. [PubMed: 18290061]

7. Glaunés J, Vaillant M, Miller MI. Landmark matching via large deformation diffeomorphisms on the sphere. J. Math. Imaging Vis. 2004; 20(1–2):179–200.

8. Avants BB, Gee JC. Shape averaging with diffeomorphic flows for atlas creation. ISBI. 2004:324–327.

9. Thompson PM, Toga AW. A surface-based technique for warping 3-dimensional brain. IEEE Transactions on Medical Imaging. 1996; 15(4):1–16.

10. Downs, JH.; Lancaster, JL.; Fox, PT. Brain Warping. San Diego, CA: Academic Press; 1999. Surface based spatial normalization using convex hulls.

11. Hartkens T, Hill D, Castellano-Smith AD, Hawkes D, Maurer C, Martin A, Hall WH, Liu CT. Using points and surfaces to improve voxel-based non-rigid registration. MICCAI. 2002:565–572.

12. Davatzikos C, Prince J, Bryan R. Image registration based on boundary mapping. IEEE Transactions on Medical Imaging. 1996; 15(1):112–115. [PubMed: 18215894]

13. Davatzikos C, Prince J. Brain image registration based on curve mapping. IEEE Workshop Biomedical Image Anal. 1994:245–254.

14. Collins, DL.; Goualher, GL.; Evans, AC. MICCAI. London, UK: Springer-Verlag; 1998. Non-linear cerebral registration with sulcal constraints; p. 974-984.

15. Cachier P, Mangin JF, Pennec X, Rivière D, Papadopoulos-Orfanos D, Régis J, Ayache N. Multisubject non-rigid registration of brain mri using intensity and geometric features. MICCAI. 2001:734–742.

16. Joshi SC, Miller MI. Landmark matching via large deformation diffeomorphisms. IEEE Transactions on Image Processing. 2000 Aug; 9(8):1357–1370. [PubMed: 18262973]

17. Gerig G, Joshi S, Fletcher T, Gorczowski K, Xu S, Pizer SM, Styner M. Statistics of population of images and its embedded objects: Driving applications in neuroimaging. ISBI. 2006 Apr.:1120–1123.

18. Liu T, Shen D, Davatzikos C. Deformable registration of cortical structures via hybrid volumetric and surface warping. NeuroImage. 2004; 22(4):1790–1801. [PubMed: 15275935]

19. Hurdal MK, Stephenson K, Bowers PL, Sumners DWL, Rottenberg DA. Coordinate system for conformal cerebellar flat maps. NeuroImage. 2000; 11:S467.

20. Joshi AA, Leahy RM, Thompson PM, Shattuck DW. Cortical surface parameterization by p-harmonic energy minimization. ISBI. 2004:428–431.

21. Fischl B, Sereno MI, Tootell RBH, Dale AM. High-resolution inter-subject averaging and a coordinate system for the cortical surface. Human Brain Mapping. 1998; 8:272–284. [PubMed: 10619420]

22. Bakircioglu M, Grenander U, Khaneja N, Miller MI. Curve matching on brain surfaces using frenet distances. Human Brain Mapping. 1998; 6:329–333. [PubMed: 9788068]

23. Tosun D, Rettmann ME, Prince JL. Mapping techniques for aligning sulci across multiple brains. Medical Image Analysis. 2005; 8(3):295–309. [PubMed: 15450224]

24. Thompson PM, Wood RP, Mega MS, Toga AW. Mathematical/computational challenges in creating deformable and probabilistic atlases of the human brain (invited paper). Human Brain Mapping. 2000 Feb.9(2):81–92. [PubMed: 10680765]

25. Joshi AA, Shattuck DW, Thompson PM, Leahy RM. A framework for registration, statistical characterization and classification of cortically constrained functional imaging data. LNCS. 2005 Jul.3565:186–196.

26. Wang Y, Chiang MC, Thompson PM. Automated surface matching using mutual information applied to Riemann surface structures. MICCAI 2005, LNCS. 2005; 3750:666–674.

27. Eells J, Sampson JH. Harmonic mappings of Riemannian manifolds. Ann. J. Math. 1964:109–160.

28. Hamilton, R. Lecture Notes in Mathematics. Vol. 471. Springer; 1975. Harmonic maps of manifolds with boundary.

29. Jost, J. Riemannian geometry and geometric analysis. Springer Verlag; 2002.

30. Fardoun A, Regbaoui R. Heat flow for p-harmonic maps between compact Riemannian manifolds. Indiana Univ. Math. J. 2002; 51:1305–1320.

31. Angenent S, Haker S, Tannenbaum A, Kikinis R. Laplace-Beltrami operator and brain surface flattening. IEEE Transactions on Medical Imaging. 1999; 18:700–711. [PubMed: 10534052]

32. Kanai T, Suzuki H, Kimura F. Three-dimensional geometric metamorphosis based on harmonic maps. The Visual Computer. 1998; 14(4):166–176.

33. Tang B, Sapiro G, Caselles V. Diffusion of general data on non-flat manifolds via harmonic maps theory: The direction diffusion case. International Journal of Computer Vision. 2000; 36(2):149–161.

34. Wang Y, Gu X, Yau ST. Volumetric harmonic map. Communications in Information and Systems. 2004; 3(3):191–202.

35. Joshi AA, Shattuck DW, Thompson PM, Leahy RM. Simultaneous surface and volumetric registration using harmonic maps. Proceedings of SPIE. 2007 Feb.

36. Joshi A, Shattuck D, Thompson P, Leahy R. Simultaneous surface and volumetric brain registration using harmonic mappings. IEEE TMI. (submitted).

37. Eriksson AP, Åström K. On the bijectivity of thin plate transforms. Swedish Symposium on Image Analysis. 2005:53–56.

38. Jost J, Schoen R. On the existence of harmonic diffeomorphisms between surfaces. Invent. math. 1982; 66:353–359.

39. Shattuck DW, Leahy RM. BrainSuite: An automated cortical surface identification tool. Medical Image Analysis. 2002; 8(2):129–142. [PubMed: 12045000]

40. Joshi A, Shattuck D, Thompson P, Leahy R. A finite element method for elastic parameterization and alignment of cortical surfaces using sulcal constraints. Proc. of ISBI. 2007

41. Hermosillo G, Chefd'hotel C, Faugeras O. Variational methods for multimodal image matching. International Journal of Computer Vision. 2002 Dec; 50(3):329–343.

42. Shen D, Davatzikos C. HAMMER: Hierarchical attribute matching mechanism for elastic registration. IEEE Trans. on Med. Imag. 2002; 21(11):1421–1439.

43. Zijdenbos AP, Dawant BM, Margolin RA, Palmer A. Morphometric analysis of white matter lesions in mr images. IEEE TMI. 1994 Dec.13:716–724.

44. Leow, A.; Thompson, PM.; Protas, H.; Huang, SC. ISBI. IEEE; 2004. Brain warping with implicit representations; p. 603-606.

45. Mémoli F, Sapiro G, Thompson P. Implicit brain imaging. NeuroImage. 2004; 23(1):S179–S188. [PubMed: 15501087]

46. Camion V, Younes L. Geodesic interpolating splines. Lecture Notes in Computer Science. 2001:513–527.

47. Ge Y, Fitzpatrick JM, Kessler RM, Jeske-Janicka M, Margolin RA. Intersubject brain image registration using both cortical and subcortical landmarks. Proc. SPIE. 1995 May.2434:81–95.

48. Christensen GE. Consistent linear-elastic transformations for image matching. Lecture Notes in Computer Science. 1999; 1613:224–237.

49. Mémoli F, Sapiro G, Osher S. Solving variational problems and partial differential equations mapping into general target manifolds. J. Comput. Phys. 2004; 195(1):263–292.

50. Christensen GE, Joshi SC, Miller MI. Volumetric transformation of brain anatomy. IEEE TMI. 1997 Dec; 16(6):864–877.
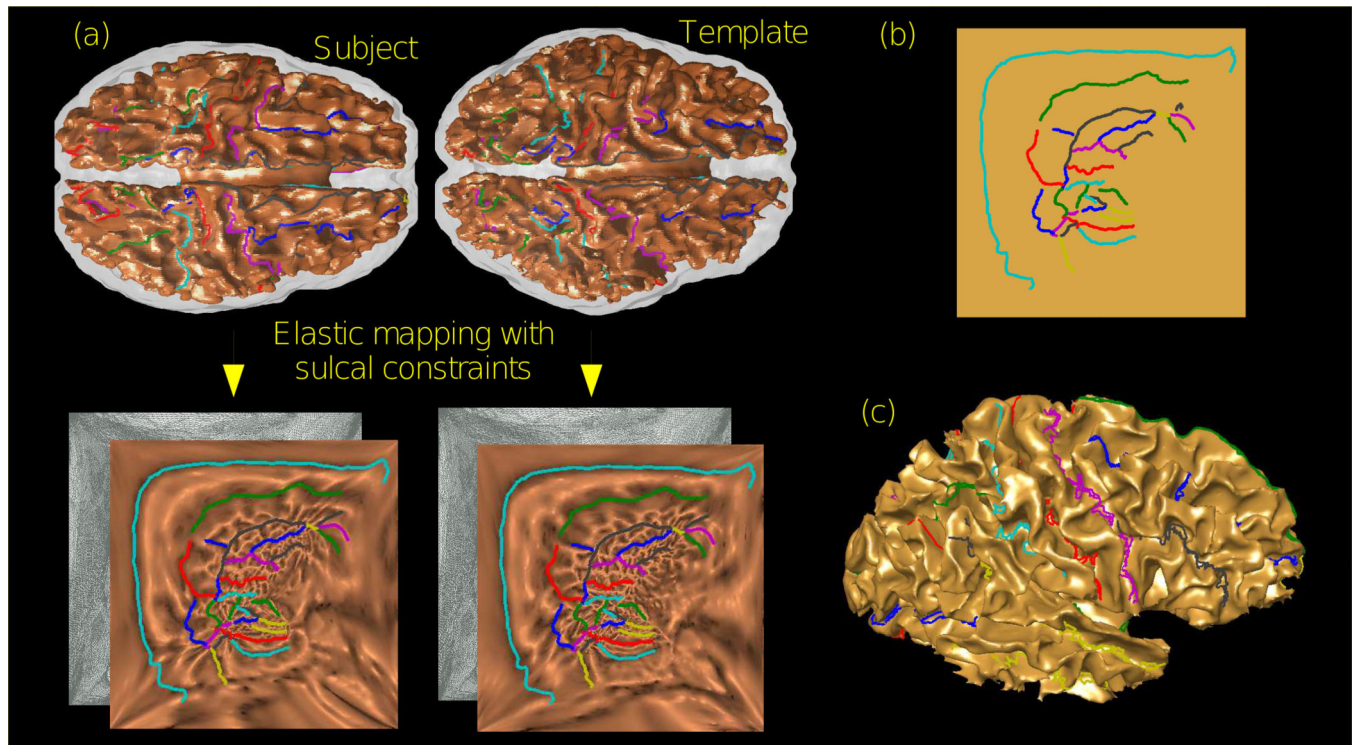
Fig. 1.
(a) Our surface registration method involves simultaneous flattening and sulcal landmark alignment of the two cortical surfaces, which produces accurate sulcal mapping from one cortex to another. The outer grey matter/CSF surface is shown in semi-transparent grey color and the inner grey/CSF surface is opaque. Shown below are flat maps of a single hemisphere for the inner cortical surface of the two brains. (b) Mapping of the aligned sulci in the flat space and (c) sulci mapped back to the inner cortical surface of the template.
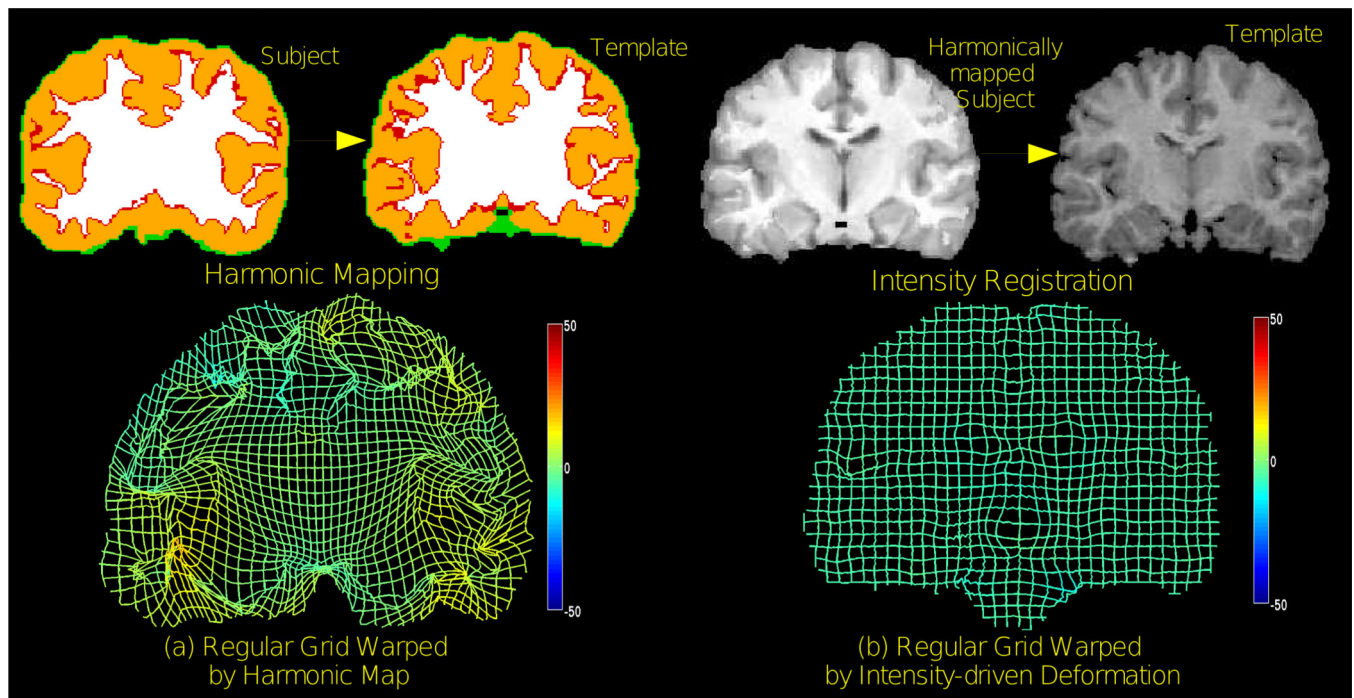
Fig. 2.
(a) Illustration of the extrapolation of the surface mapping to the 3D volume by harmonic mapping. The pairs of surfaces are shown in red and green. The deformation field is represented by placing a regular grid in the central coronal slice of the brain and deforming it according to the harmonic map. The projection of this deformation onto a 2D plane is shown with the in-plane value encoded according to the adjacent color bar. (b) The result of harmonic mapping and linear elastic refinement of the subject brain to the template brain. Note that the inner and outer cortical surfaces, by constraint, are exactly matched. The linear elastic refinement produces an approximate match between subcortical structures. The deformation field here shows the result of cortically constrained intensity-driven refinement. Note that the deformations are zero at the boundary and nonzero in the vicinity of the ventricles, thalamus and other subcortical structures.
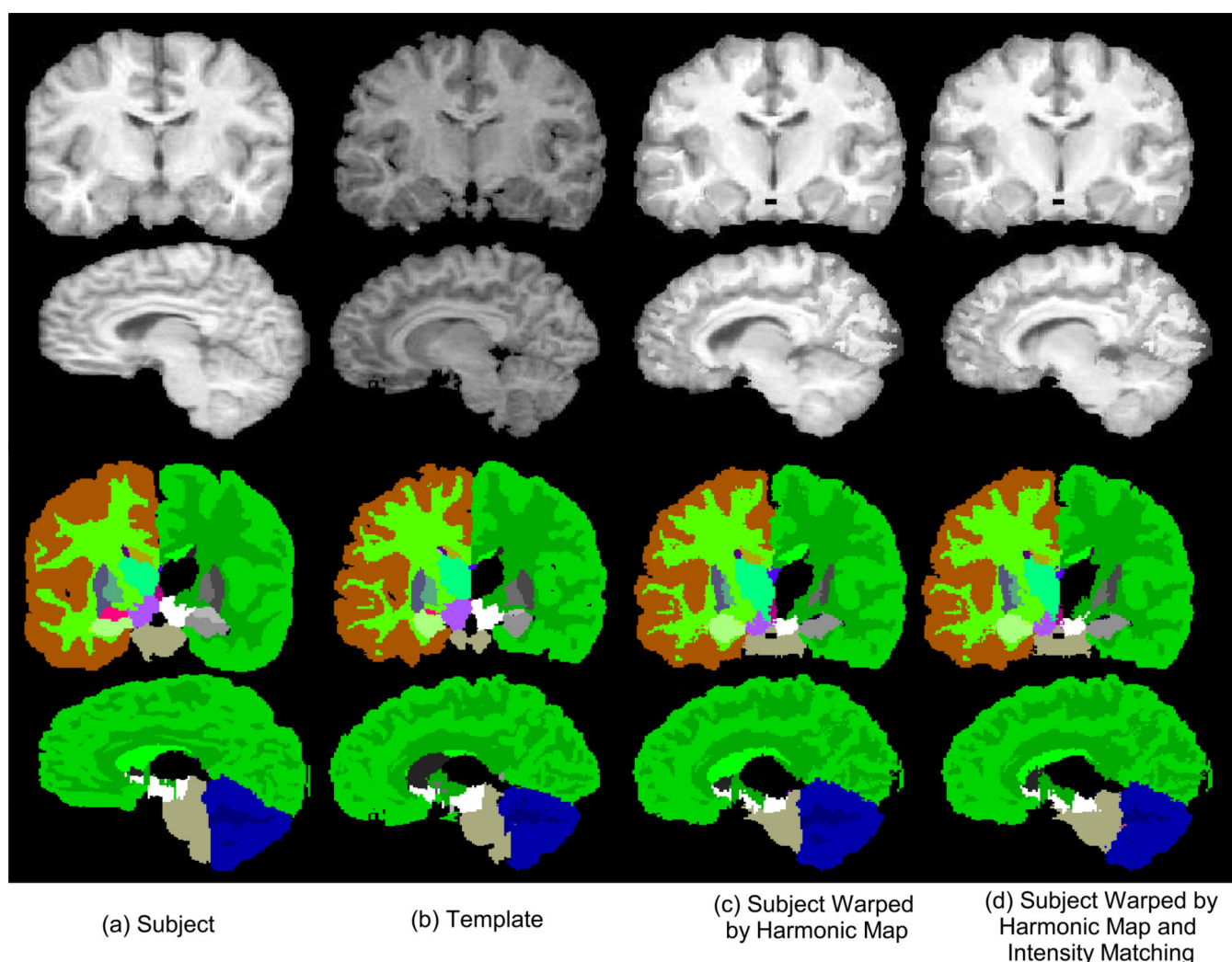
(a) Subject   (b) Template   (c) Subject Warped by Harmonic Map   (d) Subject Warped by Harmonic Map and Intensity Matching

Fig. 3.
Examples of surface constrained volumetric registration. (a) Original subject volume; (b) template; (c) registration of subject to template using surface constrained harmonic mapping, note that the cortical surface matches that of the template; (d) intensity-based refinement of the harmonic map of subject to template

Table 1

Comparison of Dice coefficients and RMS errors in sulci

Subcortical Structure	AIR	HAMMER	Harmonic	Harmonic with intensity
Left Thalamus	0.7943	0.7365	0.6852	0.7163
Left Caudate	0.3122	0.5820	0.5036	0.6212
Left Putamen	0.6136	0.5186	0.4040	0.4700
Left Hippocampus	0.3057	0.6837	0.5661	0.5918
Right Thalamus	0.7749	0.8719	0.6645	0.7291
Right Caudate	0.3232	0.8107	0.4607	0.5474
Right Putamen	0.5370	0.6759	0.5229	0.5862
Right Hippocampus	0.3373	0.5974	0.5877	0.6988
Left Cerebral WM	0.5826	0.7858	0.9029	0.9118
Left Cerbral GM	0.6233	0.8388	0.9094	0.9117
Left Cerebellum WM	0.4092	0.6170	0.5333	0.6793
Left Cerebellum GM	0.5246	0.8597	0.7857	0.8227
Right Cerebral WM	0.5897	0.7938	0.9014	0.9113
Right Cerbral GM	0.6048	0.7208	0.9022	0.9050
Left Cerebellum WM	0.3686	0.5763	0.6474	0.6721
Left Cerebellum GM	0.5252	0.8535	0.8303	0.8604
RMS Error in Sulci	11*mm*	11.5*mm*	2.4*mm*	2.4*mm*